ОБЪЕДИНЕННЫЙ
ИНСТИТУТ
ЯДЕРНЫХ
ИССЛЕДОВАНИЙ

Дубна

E2-98-52

A.A.Izmest'ev, G.S.Pogosyan, A.N.Sissakian, P.Winternitz*

CONTRACTIONS OF LIE ALGEBRAS AND SEPARATION OF VARIABLES. THE n-DIMENSIONAL SPHERE

Submitted to «Journal of Mathematical Physics»

*Centre de recherches mathématiques, Université de Montréal, C.P. 6128, succ. Centre Ville Montréal, Québec H3C 3J7 Canada

1998

1 Introduction

The purpose of this article is to use Lie algebra contractions to relate the separation of variables in Helmholtz equations on n-dimensional spheres S_n and on the Euclidean spaces E_n. An earlier article [1] was devoted to the case $n = 2$. It was shown that spherical coordinates on S_2 can be contracted either to polar or Cartesian ones on E_2. Elliptic coordinates on S_2 were contracted to elliptic, parabolic and Cartesian ones on E_2.

The more complicated case of contractions from a two-dimensional Lorentzian hyperboloid H_2 to E_2 has also been studied [2].

Here we are interested in the case of S_n for arbitrary n, but will only consider the simplest types of coordinates, the so-called subgroup type coordinates [3, 4, 5, 6, 7, 8]. For S_n these are polyspherical coordinates introduced by Vilenkin [9, 10] and described by the "method of trees" [9, 10, 11, 12, 13]. Trees, or "clusters" can of course also be introduced to describe subgroup type coordinates in E_n and we shall show how "trees" on S_n are related to "clusters" on E_n via the group contraction $O(n+1) \to E(n)$.

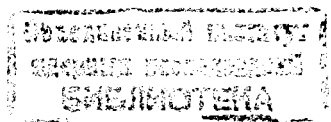

At least two definitions of Lie algebra contractions exist in the literature. The original Inönü-Wigner contractions [14, 15, 16] can be viewed as singular changes of bases. The more recent "graded contractions" [17, 18, 19, 20, 21, 22, 23] are obtained as deformations of the original Lie algebra via modifications of the commutation relations, preserving a given grading of the Lie algebra. In many cases, though not all, the two concepts are equivalent [23]. In particular, the contractions considered in this article are simultaneously Inönü-Wigner and Z_2-graded ones.

Our main tool for dealing with contractions is the concept of "analytic contractions", already introduced in Ref. [1]. The generators of the original Lie algebra, in our case $o(n+1)$, are written as differential operators, involving the contraction parameters, in our case the radius R of the sphere. The parametrization must be such that in the contraction limit, in which the $o(n+1)$ algebra contracts to the $e(n)$ one, the generators themselves as differential operators, contract into generators of $e(n)$.

As motivation for this study we mention first of all the theory of special functions. Indeed contractions relate two different groups and their homogeneous spaces. They relate separable coordinates in these two spaces, the separated equations and their solutions. The contractions will thus in particular provide asymptotic formulas and other relations between special functions.

Other applications concern relations between integrable systems in different spaces, in particular on spheres S_n and Euclidean spaces E_n. Indeed, each separable system can be extended by adding a potential that allows separation. The corresponding Hamiltonian systems will be integrable both on S_n and E_n, since they will also have n integrals of motion in involution. Again the contractions relate the S_n and E_n integrable systems and their solutions.

In Section 2 we review some known results on the method of trees for S_n [9, 10, 11, 12, 13]. We introduce $O(n)$ subgroup diagrams and relate them to the tree diagrams. Section 3 is devoted to separation of variables in Euclidean spaces E_n. We introduce $E(n)$ subgroup diagrams, E_n "cluster" diagrams and relate them. Beltrami coordinates are used in Section 4 to introduce the radius of the sphere into the expressions for the elements of the $o(n+1)$ Lie algebras. This provides the tools for an analytical realization of the Lie algebra contraction $o(n+1) \to e(n)$. The contraction of the coordinate systems and the complete sets of commuting operators is presented in Section 5. Finally, the asymptotic formulas representing contractions of solutions of Laplace-Beltrami equation on S_n to those of the Helmholtz equation on E_n are presented in Section 6.

2 Subgroup type coordinates and the method of trees

2.1 Subgroups of Lie groups and Separable Coordinates

We shall make use of an algebraic approach to separating variables in Helmholtz (and Hamilton-Jacobi) equations in Riemannian and pseudo-Riemannian spaces that are homogeneous spaces for some Lie group G [3, 4, 5, 6, 7, 8].

The equation that we are interested in can be written as

$$\Delta_{LB}\Psi = E\Psi, \quad \Delta_{LB} = \frac{1}{\sqrt{g}}\frac{\partial}{\partial\xi^i}\sqrt{g}g^{ij}\frac{\partial}{\partial\xi^j}, \quad g = |\det g_{ij}|, \tag{2.1}$$

where g_{ij} is the metric tensor written in the considered coordinates ξ_i. The space M can be identified with some factor space $M \sim G/G_0$, where G_0 is the isotropy group of the origin.

The separated solutions of the eq. (2.1) are simultaneous eigenfunctions of some complete set of n commuting operators Y_a (including the Laplace-Beltrami operator). We thus have:

$$Y_a\Psi = \lambda_a\Psi, \quad \Psi = \prod_{i=1}^{n}\Psi_i(\zeta_i;\lambda_1,\lambda_2,\ldots,\lambda_n). \tag{2.2}$$

The operators Y_a are second order operators in the enveloping algebra of the Lie algebra of the isometry group G. Thus we have a Lie algebra L with basis $L \sim \{X_1,\ldots,X_N\}$ and put

$$Y_a = A^a_{ik}X_iX_k, \quad [Y_a,Y_b] = 0, \quad A^a_{ik} = A^a_{ki}; \quad a = 1,2,\ldots,n. \tag{2.3}$$

The commuting sets of operators $\{Y_1,\ldots,Y_n\}$ can be classified into conjugacy classes under the action of the group G. Mutually conjugate sets provide equivalent systems of coordinates, transformed amongst each other by the group G.

A classification of the sets $\{Y_a\}$ provides a classification of coordinate systems. The essential properties of the coordinate systems are related to properties of the operators Y_a. In particular, ignorable coordinates [24] ξ_j, (i.e. coordinates that do not figure in the metric tensor g_{ik}), are associated with operators Y_j that are squares of the elements of the Lie algebra

$$Y_j = \left\{\sum_{k=1}^{N}a_{jk}X_k\right\}^2 = \frac{\partial^2}{\partial\alpha_j^2}. \tag{2.4}$$

Hence, maximal Abelian subalgebras [25, 26, 27, 28, 29, 30, 31] of the algebra L will provide maximal sets of ignorable variables.

Particularly simple coordinate systems are obtained if all operators Y_a in a given set are either squares of elements in the Lie algebra L, as in eq. (2.4), or Casimir operators of subalgebras of L. Such coordinate systems have been called **subgroup type coordinates** [6]. Thus, consider a chain of subalgebras

$$L \supset L_1 \supset L_2 \supset \cdots \supset L_M, \tag{2.5}$$

such that each subalgebra L_j has at least one second order Casimir operator (second order operator in the center of the enveloping algebra of L_j). Subgroup type coordinates are obtained if the chain of subalgebras provides n linearly independent second order operators. They will automatically commute amongst each other.

In this article we restrict our attention to subgroup type coordinates on spheres S_n and Euclidean spaces E_n. We mention that on S_2 precisely two types of separable coordinates exist. Spherical coordinates are subgroup type, the subgroup chain being $O(3) \supset O(2)$. Elliptic coordinates are not subgroup type. On S_3 six separable coordinate systems exist [6, 32, 33], two of them subgroup type, corresponding to the chain $O(4) \supset O(3) \supset O(2)$ and $O(4) \supset O(2) \otimes O(2)$ respectively. For E_3 three out of eleven separable coordinate systems are of the subgroup type: Cartesian, cylindrical and spherical.

A graphical method, called the "method of trees" has been developed to treat subgroup type coordinates on real and complex spheres [9, 10, 11, 12, 13]. We will reproduce some of the relevant results for **real** spheres S_n in the following subsection, and then extend them to analyze subgroup type coordinates on E_n. Moreover, we will connect the tree diagrams with subgroup diagrams, introduced below.

2.2 Subgroup Type Coordinates on S_n and the Method of Trees

Let us consider the Lie algebra $o(n+1)$ and use the standard basis of operators on S_n:

$$\begin{aligned} L_{ik} &= (u_i\partial_k - u_k\partial_i)\,; \\ [L_{ij}, L_{rs}] &= -g_{js}L_{ir} - g_{ir}L_{js} + g_{jr}L_{is} + g_{is}L_{jr}, \quad 0 \le i,k,j,r,s \le n. \end{aligned} \tag{2.6}$$

Let us now consider the defining representation of $o(n+1)$ by matrices

$$X \in \mathcal{R}^{(n+1)\otimes(n+1)}, \quad X^T + X = 0, \tag{2.7}$$

acting on the space $\mathcal{R}^{(n+1)}$. Maximal reducibly imbedded subalgebras of $o(n+1)$ will leave some vector subspace of $\mathcal{R}^n$ invariant. All subalgebras of this type have the form

$$o(n+1) \supset o(n_1) \oplus o(n_2), \quad n_1 + n_2 = n+1, \quad n_1 \ge n_2 \ge 2, \quad \text{or} \quad o(n+1) \supset o(n). \tag{2.8}$$

Maximal irreducibly imbedded subalgebras also exist, e.g. $u(n) \subset o(2n)$ or $g_2 \subset o(7)$, but they will not be needed here.

Chains of mutually maximally imbedded subalgebras are obtained by further splitting $o(n_1)$ and $o(n_2)$ into pairs of algebras, till we end the chain with one-dimensional subalgebras $o(2)$ (we drop all the $o(1) \sim \{0\}$ algebras). We shall describe subalgebra chains by subalgebra diagrams (or equivalently subgroup diagrams). Each $O(k)$ subgroup is represented by a circle with the corresponding number k in it. All subgroup diagrams of this type are shown on Fig.1 for $n \le 5$. Their recursive character is obvious: different subgroup diagrams for a given $O(n)$ correspond to different flags of invariant subspaces of $\mathcal{R}$.

The subgroup diagrams are closely related to the tree diagrams of Vilenkin [9, 10], describing polyspherical coordinates on S_n. On Fig.1 we associate a tree diagram with each subgroup diagram for $2 \le n \le 5$. Families of different, but topologically equivalent trees are associated with the same subgroup diagram. They are obtained either by permuting the end points, corresponding to the coordinates, or equivalently, by rotating branches around branching points on the tree. All different trees, including equivalent ones, are shown for S_2, S_3, S_4 on Fig.2.

The tree diagrams are best described in the original article [9] and the book [13]. Together with the subgroup diagrams described above, they provide a tool for writing coordinates on S_n, complete sets of commuting operators and their eigenvalues, and separated solutions of the Helmholtz equation.

Let us recall some basic facts here, using the example of a specific tree, namely that on Fig.3 for S_7. On Fig.3 a we give the corresponding $O(8)$ subgroup diagram. The actual S_7 tree is on Fig.3b., Fig.3c and 3d refer to the $E(7)$ group and E_7 space (after contraction) and will be used below.

Each end point on the tree of Fig.3b corresponds to a Cartesian coordinate in the ambient space $\mathcal{R}^8$. At each branching point we introduce an angle θ_i. We move along the tree from the ground upwards to a specific coordinate u_i. At each branching point we write $\cos\theta_n$ if we go to the left, $\sin\theta_n$ if we go to the right. The polyspherical coordinates corresponding to Fig.3b hence are

$$\begin{aligned} u_0 &= R\cos\theta_1\cos\theta_2\cos\theta_3, & u_4 &= R\sin\theta_1\cos\theta_5\cos\theta_6\cos\theta_7, \\ u_1 &= R\cos\theta_1\cos\theta_2\sin\theta_3, & u_5 &= R\sin\theta_1\cos\theta_5\cos\theta_6\sin\theta_7, \\ u_2 &= R\cos\theta_1\sin\theta_2\cos\theta_4, & u_6 &= R\sin\theta_1\cos\theta_5\sin\theta_6, \\ u_3 &= R\cos\theta_1\sin\theta_2\sin\theta_4, & u_7 &= R\sin\theta_1\sin\theta_5. \end{aligned} \tag{2.9}$$

The complete set of 7 commuting operators is also read off from the tree diagram, or from the subgroup one. We have:

$$\begin{aligned} &Y_3 = L_{01}^2, \quad Y_4 = L_{23}^2, \quad Y_7 = L_{45}^2, \quad Y_6 = L_{45}^2 + L_{56}^2 + L_{46}^2, \\ &Y_2 = \sum_{0\le i<k\le 3} L_{ik}^2, \quad Y_5 = \sum_{4\le i<k\le 7} L_{ik}^2, \quad Y_1 = \sum_{0\le i<k\le 7} L_{ik}^2. \end{aligned} \tag{2.10}$$

We see that Y_3, Y_4 and Y_7 are Casimir operators of $o(2)$ algebras, Y_6 of an $o(3)$ one, Y_2 and Y_5 correspond to $o(4)$ algebras and Y_1 is the original $o(8)$ Casimir operator. More generally, each circle in the subgroup chain provides the Casimir operator of the corresponding $o(k)$ to the set $\{Y_a\}$.

To each branching point on the tree diagram, or each circle on the subgroup diagram, we also associate a quantum number l_j, (see Fig.3b for a specific case). It will determine the eigenvalue λ of the corresponding $o(k)$ invariant operator according to the formula

$$Y_j\Psi = \Delta_{LB}\Psi = -l_j(l_j + k - 2)\Psi, \tag{2.11}$$

where k is the dimension of the ambient space above the corresponding vertex on the tree (the same k as in $O(k)$). The numbers l_j are nonnegative integers, labelling irreducible representations of $O(k)$ for $k \geq 3$. For $k = 2$, i.e. the group $O(2)$ we have: $l_j = 0, \pm 1, \pm 2, \ldots$.

2.3 The Separated Eigenfunctions for S_n

To specify the separated wave function

$$\Psi = \Pi_{k=1}^{n}\Psi_k(\theta_k) \tag{2.12}$$

on S_n, we follow Refs. [9, 10, 11, 12, 13] and introduce four types of vertices, or "cells" on a tree, as illustrated on Fig.4. The first row, diagrams 1a, ..., 1c, contains elementary S_n cells. The second row, 2a, ..., 2c contains E_n cells, obtained after a contraction, and will be discussed below in Section 6.1. The dashed lines in row 1 will also be explained below. A circle on diagrams 1a, ... 1c denotes a "closed" end, i.e. one that leads to further branches. An open end (no circle) leads directly to a coordinate. E.g., on Fig.3 angles θ_3, θ_4 and θ_7 correspond to cells of type "a", θ_5 and θ_6 to cells of type "b'", and θ_1, θ_2 to cells of type "c". The angles in the polyspheric coordinate systems satisfy

$$0 \leq \theta_{\rm a} < 2\pi, \quad 0 \leq \theta_{\rm b} \leq \pi, \quad -\pi/2 \leq \theta_{\rm b'} \leq \pi/2, \quad 0 \leq \theta_{\rm c} \leq \pi/2. \tag{2.13}$$

The following numbers are associated with each cell: m, l, l_β, l_α are related to the separation constant corresponding to each vertex, S_α = number of vertices above vertex l_α, S_β = number of vertices above vertex l_β. The numbers m, l, l_β, l_α are all integers, labeling representations of the corresponding rotation subgroup in the chain, i.e. angular momentum type quantum numbers. We have:

$$\Delta + c = n' - 2 \tag{2.14}$$

where n' is the number of endpoints u_i connected to the vertex θ_j and c is the number of vertices above and to the left of vertex $\theta_{\rm b'}$ or $\theta_{\rm c}$.

Each vertex and each angle θ_i provides a "building block" $\Psi_i(\theta_i)$ for the wave function $\Psi(\theta_1, \ldots, \theta_n)$ of eq. (2.12). Specifically we have:

Cell of type a:

$$\Psi_m(\theta_{\rm a}) = \frac{1}{\sqrt{2\pi}}e^{im\theta_{\rm a}}; \quad m = 0, \pm 1, \pm 2, \ldots, \ 0 \leq \theta_{\rm a} < 2\pi. \tag{2.15}$$

Cell of type b:

$$\Psi^{\alpha}_{n,l_\beta}(\theta_{\rm b}) = N^{\alpha,\alpha}_n(\sin\theta_{\rm b})^{l_\beta}P^{(\alpha,\alpha)}_n(\cos\theta_{\rm b}), \tag{2.16}$$
$$n = l - l_\beta, \ \alpha = l_\beta + \frac{S_\beta}{2}, \ n = 0, 1, 2, \ldots, \ 0 \leq \theta_{\rm b} \leq \pi.$$

where $P^{(\alpha,\beta)}_n(x)$ is a Jacobi polynomial.

Cell of type b':

$$\Psi^{\beta}_{n,l_\alpha}(\theta_{\rm b'}) = N^{\beta,\beta}_n(\cos\theta_{\rm b'})^{l_\alpha}P^{(\beta,\beta)}_n(\sin\theta_{\rm b'}); \tag{2.17}$$
$$n = l - l_\alpha, \ \beta = l_\alpha + \frac{S_\alpha}{2}, \ n = 0, 1, 2, \ldots, \ -\pi/2 \leq \theta_{\rm b'} \leq \pi/2.$$

Cell of type c:

$$\Psi^{\alpha,\beta}_{n,l_\beta,l_\alpha}(\theta_{\rm c}) = 2^{(\alpha+\beta)/2+1}N^{\alpha,\beta}_n(\sin\theta_{\rm c})^{l_\beta}(\cos\theta_{\rm c})^{l_\alpha}P^{(\alpha,\beta)}_n(\cos 2\theta_{\rm c}); \tag{2.18}$$
$$n = \frac{l - l_\alpha - l_\beta}{2}, \ \alpha = l_\beta + \frac{S_\beta}{2}, \ \beta = l_\alpha + \frac{S_\alpha}{2}, \ n = 0, 1, 2, \ldots, \ 0 \leq \theta_{\rm c} \leq \pi/2.$$

The normalization constants are:

$$N^{\alpha,\beta}_n = \sqrt{\frac{(2n + \alpha + \beta + 1)\Gamma(n + \alpha + \beta + 1)n!}{2^{\alpha+\beta+1}\Gamma(n + \alpha + 1)\Gamma(n + \beta + 1)}}. \tag{2.19}$$

We mention that the wave functions (2.16) and (2.17) can also be expressed in terms of Gegenbauer polynomials, using the formula [38]:

$$C^{\lambda}_n(x) = \frac{\Gamma(2\lambda + n)\Gamma(\lambda + 1/2)}{\Gamma(2\lambda)\Gamma(\lambda + n + 1/2)}P^{(\lambda-1/2,\lambda-1/2)}_n(x). \tag{2.20}$$

3 Subgroup type coordinates on E_n and cluster diagrams

Let us now consider the Euclidean Lie algebra $e(n)$ with a basis

$$L_{ik} = x_i\partial_{x_k} - x_k\partial_{x_i}, \quad p_i = \partial_{x_i}, \quad i, k = 1, 2, \ldots, n. \tag{3.1}$$

The commutation relations are as in eq. (2.6), together with

$$[p_j, L_{ik}] = \delta_{ji}p_k - \delta_{jk}p_i, \quad [p_i, p_k] = 0. \tag{3.2}$$

Subalgebra chains (2.5) will include Euclidean subalgebras $e(k)$ and rotation subalgebras $o(k)$. A possible link in a subalgebra chain is:

$$e(n) \supset e(n_1) \oplus e(n_2), \quad n_1 + n_2 = n,\ n_1 \geq n_2 \geq 1. \tag{3.3}$$

The Casimir operator of $e(n)$ is:

$$\Delta_n = p_1^2 + p_2^2 + \cdots + p_n^2. \tag{3.4}$$

Hence we have $\Delta_n = \Delta_{n_1} + \Delta_{n_2}$ in the chain and only one of the Euclidean subalgebras (3.3) provides a new invariant operator, say $e(n_2)$. Alternatively, Δ_{n_1} and Δ_{n_2} can replace Δ_n. A further possible link in a chain is:

$$e(n) \supset o(n), \quad n \geq 2, \tag{3.5}$$

where $o(n)$ will provide a new (with respect to $e(n)$) invariant operator.

As in the case of the $O(n)$ group we will introduce diagrams for the $E(n)$ group to illustrate subgroup chains and subgroup type coordinate systems on E_n Euclidean spaces. We shall use rectangles ("boxes") to denote $E(k)$ groups (or $e(k)$ algebras) and circles to denote $O(k)$ groups (or $o(k)$ algebras). As an example we give all subgroup chains for $E(n)$, $1 \leq n \leq 4$ on Fig.5. Maximality requires that as we go from one level to a higher one, we obey the following rules:

1. From a rectangle representing $e(n)$, we can go to two rectangles (see eq. (3.3)), representing $e(n_1) \oplus e(n_2)$, with $n_1 + n_2 = n$, $n_1 \geq n_2 \geq 1$, or to a circle (see eq. (3.5)), representing $o(n)$ (same n as in the rectangle).

2. From a circle representing $o(n)$ we can go to two circles, representing $o(n_1) \oplus o(n_2)$, $n_1 + n_2 = n$, $n_1 \geq n_2 \geq 2$, or to one circle, representing $o(n-1)$, $n \geq 3$.

Now let us consider subgroup type coordinates on the Euclidean space E_n and introduce diagrams to represent them. We shall call them "cluster diagrams" and they will consist of individual trees of the $O(k)$ type with a tree "trunk" added, or isolated "trunks", or of clusters of trees with trunks and isolated trunks. The E_n cluster diagrams are simpler than the $E(n)$ subgroup diagrams, since $E(k)$ subgroups that do not contribute new invariant operators will be omitted.

All clusters for E_n, $1 \leq n \leq 4$, are also shown on Fig.5. An isolated trunk corresponds to a Cartesian coordinate. A trunk with further branches above it corresponds to a radial coordinate r satisfying $0 \leq r < \infty$. The tree above the trunk is treated exactly as in the case of polyspheric coordinates on S_n spheres.

As an example let us consider the diagrams on Fig.3d, the coordinates in E_7 are:

$$\begin{aligned} x_1 &= z, & x_4 &= r_2\cos\theta_5\cos\theta_6\cos\theta_7, \\ x_2 &= r_1\cos\theta_4, & x_5 &= r_2\cos\theta_5\cos\theta_6\sin\theta_7, \\ x_3 &= r_1\sin\theta_4, & x_6 &= r_2\cos\theta_5\sin\theta_6, \\ & & x_7 &= r_2\sin\theta_5. \end{aligned} \tag{3.6}$$

The prescriptions for writing the complete sets of commuting operators, eigenvalues and eigenfunctions are now quite simple.

To each tree trunk we associate an M- dimensional Laplace operator, where M is the number of end points (Cartesian coordinates) above the trunk. We also associate a number $k \in \mathbf{R} > 0$ with each trunk. The corresponding radial eigenfunction (normalized to the delta function: $\delta(k'-k)$) is:

$$\begin{aligned} \Psi_{kl}(r) &= \sqrt{\frac{k}{r^{M-2}}}J_{l+(M-2)/2}(kr), & M \geq 2, \\ \Psi_k(z) &= \frac{e^{ikz}}{\sqrt{2\pi}}, & M = 1. \end{aligned} \tag{3.7}$$

The angular part of the eigenfunctions is written following the rules for S_n spheres, as are the invariant operators and their eigenvalues.

For the example of Fig.3c, 3d the invariant operators are:

$$\begin{gathered} Y_1 = p_1^2, \quad Y_2 = p_2^2 + p_3^2, \quad Y_3 = p_4^2 + p_5^2 + p_6^2 + p_7^2, \quad Y_4 = L_{23}^2, \\ Y_5 = L_{45}^2, \quad Y_6 = L_{45}^2 + L_{56}^2 + L_{46}^2, \quad Y_7 = \sum_{4\leq i<k\leq 7} L_{ik}^2. \end{gathered} \tag{3.8}$$

We note that the Laplace operator on E_7 does not figure explicitly, it is equal to

$$\Delta = \sum_{i=1}^{7} p_i^2 = Y_1 + Y_2 + Y_3. \tag{3.9}$$

4 Contractions of the Lie Algebra and Casimir Operator

Let us consider the n-dimensional sphere S_n:

$$u_0^2 + \sum_{\nu=1}^{n} u_\nu^2 = \sum_{\mu,\nu=0}^{n} g_{\mu\nu}u_\mu u_\nu = R^2, \quad R^2 > 0. \tag{4.1}$$

where u_μ are Cartesian coordinates in the Euclidean ambient space E_{n+1} and the metric tensor in this case has the form: $g_{\mu\nu} = \mathrm{diag}(1, 1, \ldots, 1)$. The isometry group

is $O(n+1)$. We choose a standard basis $L_{\mu\nu}$ for the Lie algebra $o(n+1)$ as in eq. (2.6).

The Laplace-Beltrami operator on S_n is:

$$\Delta_{LB} = \frac{1}{R^2} \sum_{0 \le \mu < \nu \le n} L_{\mu\nu}^2. \tag{4.2}$$

We shall use R^{-1} as the contraction parameter. To realize the contraction explicitly, let us introduce Beltrami coordinates on the sphere S_n putting

$$y_i = R\frac{u_i}{u_0} = u_i \left(1 - \frac{1}{R^2}\sum_{k=1}^{n} u_k^2\right)^{-1/2}, \quad i = 1, 2, 3, \ldots, n. \tag{4.3}$$

The $O(n+1)$ generators then can be expressed as:

$$\frac{L_{0i}}{R} \equiv \pi_i = p_i + \frac{y_i}{R^2}\sum_{k=1}^{n}(y_k p_k), \tag{4.4}$$

$$L_{ik} \equiv y_i p_k - y_k p_i = y_i \pi_k - y_k \pi_i; \quad i, k = 1, 2, \ldots, n, \tag{4.5}$$

where $p_i = \partial/\partial y_i$. The commutation relations now are:

$$[L_{ik}, L_{mn}] = \delta_{km} L_{in} + \delta_{in} L_{km} - \delta_{im} L_{kn} - \delta_{kn} L_{im}, \tag{4.6}$$

$$[\pi_i, L_{kj}] = \delta_{ik}\pi_j - \delta_{ij}\pi_k, \quad [\pi_i, \pi_k] = \frac{L_{ik}}{R^2}, \tag{4.7}$$

so that for $R \to \infty$ the $o(n+1)$ algebra contracts to the Euclidean $e(n)$ one. The Beltrami coordinates y_i (4.3) contract to Cartesian coordinates on E_n and we have:

$$y_i \to x_i, \quad \pi_i \to p_i = \frac{\partial}{\partial x_i}, \tag{4.8}$$

so that the rotation generators L_{0i} go into the translations p_i.

The $o(n+1)$ Laplace-Beltrami operator (2.1) contracts to the $e(n)$ one:

$$\Delta_{\mathrm{LB}} = \sum_{i=1}^{n} \pi_i^2 + \sum_{i,k=1}^{n} \frac{L_{ik}^2}{2R^2} \to \Delta = p_1^2 + p_2^2 + \cdots + p_n^2. \tag{4.9}$$

5 Contraction and Coordinate Systems. The Graphical Method

5.1 General Formulation

We have seen that all subgroup type coordinates on a sphere S_n can be characterized by tree diagrams. Similarly, there is a one-to-one correspondence between subgroup type coordinates in a Euclidean space E_n and the cluster diagrams of Section 4.

We shall now introduce a **graphical method** for connecting the subgroup type coordinate systems on S_n and E_n and give the rules relating the coordinates, invariant operators, eigenvalues and basis functions. The relations are asymptotic ones for the radius of the sphere satisfying $R \to \infty$ and one, or more, of the angles θ_i satisfying $\theta_i \to 0$.

A general S_n tree diagram can be represented by Fig.6a. One principal branch of the tree goes from the ground to the point representing the coordinate u_0. The branches growing from this one can lead directly to a coordinate u_i, or they can branch further and lead to sets of coordinates, e.g. $\{u_{l+1}, u_{l+2}, \ldots, u_{l+k}\}$. Graphically the contraction $R \to \infty$ corresponds to the fact that we cut off the ground to u_0 branch by the dashed line on Fig.6a. The dashed line then becomes the ground for the corresponding cluster E_n diagram of Fig.6b and the ambient space coordinates $(u_0, u_1, \ldots, u_n)$ for S_n are replaced by the Cartesian coordinates $(x_1, x_2, \ldots, x_n)$. The angles $\theta_1, \theta_2, \ldots, \theta_j$ that lead to branches cut-off by the dotted line satisfy $\theta_i \to 0$ in the contraction and are replaced by radial coordinates r_i, or Cartesian coordinates x_m (if the surviving branch leads directly to a single coordinate on S_n and E_n). We have:

$$R \to \infty, \quad \theta_i \to 0, \quad R\tan\theta_i \sim R\sin\theta_i \sim R\theta_i \to r_i. \tag{5.1}$$

The individual trees in an E_n cluster correspond to $O(k)$ subgroups of $O(n)$ that survive the contraction.

All contractions of coordinate systems for S_1, S_2, and S_3 are illustrated on Fig.7. Let us run through the individual cases.

5.2 Contractions from S_1 to E_1

In the case of a one-dimensional sphere, i.e. a circle, we have only one diagram, namely No. 1 of Fig.7. In the original ambient space we have polar coordinates

$$u_0 = R\cos\theta, \quad u_1 = R\sin\theta, \tag{5.2}$$

with $0 \le \theta < 2\pi$. The Beltrami coordinate satisfies

$$y_1 = R\tan\theta \to x, \tag{5.3}$$

where x is a Cartesian coordinate on E_1.

5.3 Contractions from S_2 to E_2

In the case of the two-dimensional sphere S_2 we have two tree configurations and two types of coordinate contractions to consider, namely No. 2 and No. 3 of Fig.7.

For **diagram** No. 2 we have

$$u_0 = R\cos\theta_1, \quad u_1 = R\sin\theta_1\cos\theta_2, \quad u_2 = R\sin\theta_1\sin\theta_2, \tag{5.4}$$

where $0 \leq \theta_1 < \pi$, $0 \leq \theta_2 < 2\pi$. Introducing Beltrami coordinates and taking the appropriate limits $R \to \infty$, $\theta_1 \sim r/R$ we have:

$$y_1 = R\tan\theta_1\cos\theta_2 \to x_1 = r\cos\theta_2, \quad y_2 = R\tan\theta_1\sin\theta_2 \to x_2 = r\sin\theta_2. \tag{5.5}$$

The subgroup chain $O(3) \supset O(2)$ contracts to the Euclidean one: $E(2) \supset O(2)$; the $O(2)$ invariant and its eigenvalues m survive the contraction $L_{12}^2 \to L_{12}^2, m \to m$.

For **diagram** No. 3 on Fig.7 we have

$$u_0 = R\cos\theta_1\cos\theta_2, \quad u_1 = R\cos\theta_1\sin\theta_2, \quad u_2 = R\sin\theta_1 \tag{5.6}$$

and the Beltrami coordinates satisfy ($R \to \infty$, $\theta_1 \sim x_1/R$, $\theta_2 \sim x_2/R$)

$$y_1 = R\tan\theta_2 \to x_1, \quad y_2 = R\frac{\tan\theta_1}{\cos\theta_2} \to x_2. \tag{5.7}$$

The subgroup chain $O(3) \supset O(2)$ contracts to $E(2) \supset E(1) \otimes E(1)$ and the $O(2)$ subgroup invariant undergoes a contraction

$$\frac{Y_1}{R^2} = \frac{L_{01}^2}{R^2} = \pi_1^2 \to p_1^2. \tag{5.8}$$

5.4 Contractions from S_3 to E_3

Five types of $O(4)$ tree diagrams exist, but only four of them give different contractions.

The **diagrams** No. 4 and 4′ on Fig.7 correspond to spherical coordinates on S_3 going into spherical coordinates on E_3. For No. 4 the polyspherical coordinates are

$$\begin{aligned} u_0 &= R\cos\theta_1, & u_1 &= R\sin\theta_1\cos\theta_2, \\ u_2 &= R\sin\theta_1\sin\theta_2\cos\theta_3, & u_3 &= R\sin\theta_1\sin\theta_2\sin\theta_3\,. \end{aligned} \tag{5.9}$$

The Beltrami coordinates satisfy ($R \to \infty$, $\theta_1 \sim r/R$)

$$\begin{aligned} y_1 &= R\tan\theta_1\cos\theta_2 \to x_1 = r\cos\theta_2, \\ y_2 &= R\tan\theta_1\sin\theta_2\cos\theta_3 \to x_2 = r\sin\theta_2\cos\theta_3, \\ y_3 &= R\tan\theta_1\sin\theta_2\sin\theta_3 \to x_3 = r\sin\theta_2\sin\theta_3. \end{aligned} \tag{5.10}$$

We have $O(4) \supset O(3) \supset O(2) \to E(3) \supset O(3) \supset O(2)$ so that the $O(3) \supset O(2)$ subgroups and their invariants survive:

$$Y_1 = \mathbf{L}^2 = L_{12}^2 + L_{13}^2 + L_{23}^2 \to \mathbf{L}^2, \quad Y_2 = L_{23}^2 \to L_{23}^2 \tag{5.11}$$

The situation for diagram No. 4′ is quite analogous.

The case No. 5 on Fig.7 corresponds to spherical coordinates contracting to cylindrical ones. We have

$$\begin{aligned} u_0 &= R\cos\theta_1\cos\theta_2, \quad u_1 = R\cos\theta_1\sin\theta_2\cos\theta_3, \\ u_2 &= R\cos\theta_1\sin\theta_2\sin\theta_3, \quad u_3 = R\sin\theta_1. \end{aligned} \tag{5.12}$$

For Beltrami coordinates ($R \to \infty$, $\theta_2 \sim r/R$, $\theta_1 \sim x_3/R$) we obtain:

$$\begin{aligned} y_1 &= R\tan\theta_2\cos\theta_3 \to x_1 = r\cos\theta_3, \\ y_2 &= R\tan\theta_2\sin\theta_3 \to x_2 = r\sin\theta_3, \\ y_3 &= R\frac{\tan\theta_1}{\cos\theta_2} \to x_3 = z. \end{aligned} \tag{5.13}$$

The subgroup chain contraction is $O(4) \supset O(3) \supset O(2) \to E(3) \supset E(2) \otimes E(1) \supset O(2)$ and the subgroup invariants contract as

$$\frac{Y_1}{R^2} = \frac{1}{R^2}(L_{01}^2 + L_{02}^2 + L_{12}^2) = \pi_1^2 + \pi_2^2 + \frac{L_{12}^2}{R^2} \to p_1^2 + p_2^2, \quad Y_2 = L_{12}^2 \to L_{12}^2. \tag{5.14}$$

The diagram No. 6 on Fig.7 corresponds to the contraction of spherical coordinates to Cartesian ones. We have:

$$\begin{aligned} u_0 &= R\cos\theta_1\cos\theta_2\cos\theta_3, & u_1 &= R\cos\theta_1\cos\theta_2\sin\theta_3, \\ u_2 &= R\cos\theta_1\sin\theta_2, & u_3 &= R\sin\theta_1. \end{aligned} \tag{5.15}$$

For Beltrami coordinates after the contraction $R \to \infty$, $\theta_3 \sim x_1/R$, $\theta_2 \sim x_2/R$, $\theta_1 \sim x_3/R$ we have

$$\begin{aligned} y_1 &= R\tan\theta_3 \to x_1, \\ y_2 &= R\frac{\tan\theta_2}{\cos\theta_3} \to x_2, \\ y_3 &= R\frac{\tan\theta_1}{\cos\theta_2\cos\theta_3} \to x_3. \end{aligned} \tag{5.16}$$

The subgroup chain undergoes the contraction $O(4) \supset O(3) \supset O(2) \to E(3) \supset E(1) \otimes E(1) \otimes E(1)$ and the subgroup invariants satisfy

$$\frac{Y_1}{R^2} = \frac{1}{R^2}(L_{01}^2 + L_{02}^2 + L_{12}^2) = \pi_1^2 + \pi_2^2 = \frac{L_{12}^2}{R^2} \to p_1^2 + p_2^2, \quad \frac{Y_2}{R^2} = \frac{L_{01}^2}{R^2} = \pi_1^2 \to p_1^2. \tag{5.17}$$

Finally the diagram No. 7 of Fig.7 corresponds to polyspherical (or cylindrical) coordinates on S_3 contracting to cylindrical ones on E_3. We have:

$$\begin{aligned} u_0 &= R\cos\theta_1\cos\theta_2, & u_1 &= R\cos\theta_1\sin\theta_2, \\ u_2 &= R\sin\theta_1\cos\theta_3, & u_3 &= R\sin\theta_1\sin\theta_3. \end{aligned} \tag{5.18}$$

For the Beltrami coordinates after the contraction $R \to \infty$, $\theta_2 \sim x_1/R$, $\theta_1 \sim r/R$ we obtain:

$$\begin{aligned} y_1 &= R\tan\theta_2 \to x_1. \\ y_2 &= R\tan\theta_1 \frac{\cos\theta_3}{\cos\theta_2} \to x_2 = r\cos\theta_3, \\ y_3 &= R\tan\theta_1 \frac{\sin\theta_3}{\cos\theta_2} \to x_3 = r\sin\theta_3. \end{aligned} \tag{5.19}$$

The subgroup chain satisfies $O(4) \supset O(2) \oplus O(2) \to E(3) \supset E(2) \oplus E(1) \supset O(2)$ so that for the subgroup invariants we have:

$$\frac{Y_1}{R^2} = \frac{L_{01}^2}{R^2} = \pi_1^2 \to p_1^2, \quad Y_2 = L_{23}^2 \to L_{23}^2. \tag{5.20}$$

6 Contractions of basis functions

6.1 Contractions of functions corresponding to elementary cells

When we cut off the branches of a tree as on Fig.6, the cutting line intersects an elementary cell (see Fig.4.) at each branch. Each elementary $O(n+1)$ cell then goes into an elementary trunk for $E(n)$, as indicated by the lower row of diagrams on Fig.4.

Let us now discuss the four cases on Fig.4. The limiting procedure is always the same, namely

$$\theta_j \sim \frac{r_j}{R}, \quad l_j \sim kR, \quad R \to \infty, \quad j = \mathrm{a}, \mathrm{b}, \mathrm{b}', \mathrm{c}, \tag{6.1}$$

where r_j is the radius of the sphere that survives the contraction, i.e. corresponds to the circle on the right-hand side of the $O(n+1)$ cell and on top of the $E(n)$ trunk. Thus, for $j = \mathrm{a}$ and $j = \mathrm{b}'$ we have $r_j = x$, a Cartesian coordinate. Similarly, we have $l_\alpha = m \in \mathbf{Z}$ and also $l_\beta = m \in \mathbf{Z}$.

Let us now run through the individual cells on Fig.4.

1 Cell 1a to 2a

Using eq. (2.15) and (6.1) we have ($R \to \infty, m \sim kR, \theta \sim x/R$):

$$\lim_{R\to\infty} \frac{1}{\sqrt{2\pi}} e^{im\theta_{\mathrm{a}}} = \frac{1}{\sqrt{2\pi}} e^{ikx}.$$

2 Cell 1b to 2b

The contribution to the separated $O(n+1)$ basis function is given in eq. (2.16). Using the formula for Jacobi polynomials in the terms of the hypergeometric functions [38]

we have:

$$N_{l-l_\beta}^{l_\beta+S_\beta/2,l_\beta+S_\beta/2}(\sin\theta_{\mathrm{b}})^{l_\beta} P_{l-l_\beta}^{(l_\beta+S_\beta/2,l_\beta+S_\beta/2)}(\cos\theta_{\mathrm{b}}) = \sqrt{\frac{(2l+S_\beta+1)(l+l_\beta+S_\beta)!}{2(l-l_\beta)!}}$$
$$\cdot \frac{(\sin\theta_{\mathrm{b}})^{l_\beta}}{2^{l_\beta+S_\beta/2}\Gamma(l_\beta+S_\beta/2+1)} {}_2F_1\left(-l+l_\beta, l+l_\beta+S_\beta+1; l_\beta+\frac{S_\beta}{2}+1; \sin^2\frac{\theta_{\mathrm{b}}}{2}\right).$$

Now using the asymptotic formulas for the hypergeometric and Γ functions ($l \sim kR$, $\theta_{\mathrm{b}} \sim r/R$)

$$\lim_{R\to\infty} {}_2F_1\left(-l+l_\beta, l+l_\beta+S_\beta+1; l_\beta+\frac{S_\beta}{2}+1; \sin^2\frac{\theta_{\mathrm{b}}}{2}\right)$$
$$= {}_0F_1\left(l_\beta+\frac{S_\beta}{2}+1; -\frac{k^2r^2}{4}\right),$$
$$\lim_{|z|\to\infty} \frac{\Gamma(z+\alpha)}{\Gamma(z+\beta)} = z^{\alpha-\beta}\left(1+\frac{1}{2z}(\alpha-\beta)(\alpha+\beta-1)+O(z^{-2})\right)$$

and formula for Bessel function

$$J_\nu(z) = \left(\frac{z}{2}\right)^\nu \frac{1}{\Gamma(\nu+1)} {}_0F_1\left(\nu+1; -\frac{z^2}{4}\right)$$

we obtain:

$$\lim_{R\to\infty} \frac{1}{\sqrt{R^{S_\beta+1}}} N_{l-l_\beta}^{l_\beta+S_\beta/2,l_\beta+S_\beta/2}(\sin\theta_{\mathrm{b}})^{l_\beta} P_{l-l_\beta}^{(l_\beta+S_\beta/2,l_\beta+S_\beta/2)}(\cos\theta_{\mathrm{b}}) = \sqrt{\frac{k}{r^{S_\beta}}} J_{l_\beta+S_\beta/2}(kr).$$

3 Cell 1b′ to 2b′

The contribution of this cell to the $O(n+1)$ separated basis function is given in eq. (2.17). In order to take the contraction limit (6.1) we express the Jacobi polynomials in terms of hypergeometric functions [38]:

$$P_n^{(\alpha,\alpha)}(x) = \frac{2^{2\alpha}}{\sqrt{\pi}} \frac{\Gamma(n+\alpha+1)}{\Gamma(n+2\alpha+1)}$$
$$\times \begin{cases} (-1)^{n/2} \frac{\Gamma([n+1]/2+\alpha)}{\Gamma(n/2+1)} {}_2F_1\left(-\frac{n}{2}, \frac{n+1}{2}+\alpha; \frac{1}{2}; x^2\right), & n \text{ even}, \\ (-1)^{(n-1)/2} \frac{\Gamma(n/2+\alpha+1)}{\Gamma([n+1]/2)} 2x\, {}_2F_1\left(-\frac{n-1}{2}, \frac{n+2}{2}+\alpha; \frac{3}{2}; x^2\right), & n \text{ odd}. \end{cases}$$

In the limit $R \to \infty$ and $\theta_{\mathrm{b}'} \sim x_n/R, l \sim kR, l_\alpha \sim pR$ we have:

$$\lim_{R\to\infty} (-1)^{(l-l_\alpha)/2} N_{l-l_\alpha}^{l_\alpha+S_\alpha/2,l_\alpha+S_\alpha/2}(\cos\theta_{\mathrm{b}'})^{l_\alpha} P_{l-l_\alpha}^{(l_\alpha+S_\alpha/2,l_\alpha+S_\alpha/2)}(\sin\theta_{\mathrm{b}'})$$
$$= \sqrt{\frac{2k}{\pi k_n}} \times \begin{cases} {}_0F_1\left(\frac{1}{2}; \frac{-k_n^2x_n^2}{4}\right), \\ -i(k_nx_n) {}_0F_1\left(\frac{3}{2}; \frac{-k_n^2x_n^2}{4}\right), \end{cases}$$

where $k^2 = p^2 + k_n^2$. The ${}_0F_1(x)$ hypergeometric functions in this case are expressible in terms of $\sin k_n x_n$ and $\cos k_n x_n$ functions [38]

$$ {}_0F_1\left(\frac{1}{2}; \frac{-k_n^2 x_n^2}{4}\right) = \cos k_n x_n, \quad (k_n x_n)\, {}_0F_1\left(\frac{3}{2}; \frac{-{k_n}^2 x_n^2}{4}\right) = \sin k_n x_n, $$

and we finally have:

$$ \lim_{R\to\infty} (-1)^{(l-l_\alpha)/2} N_{l-l_\alpha}^{l_\alpha+S_\alpha/2, l_\alpha+S_\alpha/2}(\cos\theta_{b'})^{l_\alpha} P_{l-l_\alpha}^{(l_\alpha+\frac{S_\alpha}{2}, l_\alpha+\frac{S_\alpha}{2})}(\sin\theta_{b'}) $$

$$ = \sqrt{\frac{2k}{\pi k_n}} \left\{ \begin{array}{c} \cos(k_n x_n) \\ -i\sin(k_n x_n) \end{array} \right\}. $$

4 Cell 1c to 2c

The relevant basis function is given in eq. (2.18). To take the limit (6.1), $l \sim kR$, $l_\alpha \sim k_\alpha R$ and $\theta \sim r/R$, we use the equation expressing Jacobi polynomials in terms of hypergeometric functions, and take the limit leading to Bessel functions:

$$ \lim_{R\to\infty} \frac{\Gamma([l-l_\alpha-l_\beta]/2+1)}{\Gamma([l-l_\alpha+l_\beta+S_\beta]/2+1)} P_{(l-l_\alpha-l_\beta)/2}^{(l_\beta+\frac{S_\beta}{2}, l_\alpha+\frac{S_\alpha}{2})}(\cos 2\theta_c) = \lim_{R\to\infty} \frac{1}{\Gamma(l_\beta+\frac{S_\beta}{2}+1)} $$

$$ \cdot {}_2F_1\left(-\frac{l-l_\alpha-l_\beta}{2}, \frac{l+l_\alpha+l_\beta+S_\alpha+S_\beta}{2}+1; l_\beta+\frac{S_\beta}{2}+1; \sin^2\theta_c\right) $$

$$ = \frac{1}{\Gamma(l_\beta+S_\beta/2+1)} {}_0F_1\left(l_\beta+\frac{S_\beta}{2}+1; -\frac{k_\beta^2 r^2}{4}\right) = \left(\frac{2}{k_\beta r}\right)^{l_\beta+S_\beta/2} J_{l_\beta+S_\beta/2}(k_\beta r), $$

where $k_\alpha^2 + k_\beta^2 = k^2$. The final result is:

$$ \lim_{R\to\infty} \frac{2^{(l_\alpha+S_\alpha/2+l_\beta+S_\beta/2)/2+1}}{\sqrt{R^{S_\beta+1}}} N_{(l-l_\alpha-l_\beta)/2}^{l_\beta+S_\beta/2, l_\alpha+S_\alpha/2}(\sin\theta_c)^{l_\beta}(\cos\theta_c)^{l_\alpha} $$

$$ \cdot P_{(l-l_\alpha-l_\beta)/2}^{(l_\beta+S_\beta/2, l_\alpha+S_\alpha/2)}(\cos 2\theta_c) = \sqrt{\frac{2k}{r^{S_\beta}}} J_{l_\beta+S_\beta/2}(k_\beta r). $$

These contractions for basis functions of the elementary cells (1a, ..., 1c) determine the general contractions for hyperspherical functions corresponding to any tree for the sphere S_n.

6.2 Examples

The contraction formulas for basis functions of $O(3)$ were given in Ref. [1]. Here we apply the general rules to give all different S_3 and S_4 contraction diagrams on Fig.7.

The S_3 sphere

1. Polyspherical to spherical coordinates (see Fig.7(4) 7(4')) [$R \to \infty$, $J \sim kR$]

$$ \lim_{R\to\infty} \frac{1}{R} \Psi_{Jlm}(\theta_1, \theta_2, \theta_3) = \sqrt{\frac{k}{r}} J_{l+1/2}(kr) Y_{lm}(\theta_2, \theta_3). $$

where $Y_{lm}(\theta_2, \theta_3)$ is a spherical function on S_2.

2. Polyspherical to cylindrical coordinates (see Fig.7(5)) [$R \to \infty$, $J \sim kR$, $l \sim k_3/R$]

$$ \lim_{R\to\infty} \frac{(-1)^{(J-l)/2}}{\sqrt{R}} \Psi_{Jlm}(\theta_1, \theta_2, \theta_3) = \sqrt{\frac{kp}{\pi k_3}} J_{|m|}(pr) \frac{e^{im\theta_3}}{\sqrt{2\pi}} \left\{ \begin{array}{c} \cos k_3 z \\ -i\sin k_3 z \end{array} \right\}. $$

where $k^2 = k_3^2 + p^2$.

3. Polyspherical to Cartesian coordinates (see Fig.7(6)) [$R \to \infty$, $J \sim k_1 R$, $l \sim k_2/R$, $m \sim k_3 R$]

$$ \lim_{R\to\infty} (-1)^{(J-m)/2} \Psi_{Jlm}(\theta_1, \theta_2, \theta_3) = \sqrt{\frac{2}{\pi k_1 k_3}} \frac{e^{ik_1 x}}{\pi} \left\{ \begin{array}{c} \cos k_2 y \cos k_3 z \\ -i\sin k_2 y \cos k_3 z \\ -i\cos k_2 y \sin k_3 z \\ -\sin k_2 y \sin k_3 z \end{array} \right\}. $$

where $k^2 = k_1^2 + k_2^2 + k_3^2$.

4. Polyspherical (cylindrical) to cylindrical coordinates (see Fig.7(7)) [$R \to \infty$, $J \sim kR$, $m \sim k_3 R$]

$$ \lim_{R\to\infty} \frac{1}{\sqrt{R}} \Psi_{Jm_1m_2}(\theta_1, \theta_2, \theta_3) = \sqrt{\frac{k}{\pi}} J_{|m_2|}(pr) e^{ik_3 z} \frac{e^{im_2\theta_3}}{\sqrt{2\pi}}, $$

where $k^2 = k_3^2 + p^2$.

The S_4 sphere

1. Polyspherical to polyspherical coordinates (see Fig.7(8) 7(8'''))[$R \to \infty$, $J \sim kR$]

$$ \lim_{R\to\infty} \frac{1}{\sqrt{R^3}} \Psi_{Jl_1l_2m}(\theta_1, \theta_2, \theta_3, \theta_4) = \frac{\sqrt{k}}{r} J_{l_1+1}(kr) \Psi_{l_1l_2m}(\theta_2, \theta_3, \theta_4). $$

where $\Psi_{l_1l_2m}(\theta_2, \theta_3, \theta_4)$ is a hyperspherical function on S_3.

2. Polyspherical to cylindrical coordinates (see Fig.7(9)) $[R \to \infty,\ J \sim kR]$

$$\lim_{R\to\infty} \frac{1}{\sqrt{R^3}} \Psi_{Jlm_1m_2}(\theta_1,\theta_2,\theta_3,\theta_4) = \frac{\sqrt{k}}{r} J_{l+1}(kr) \Psi_{lm_1m_2}(\theta_2,\theta_3,\theta_4),$$

where $\Psi_{lm_1m_2}(\theta_2,\theta_3,\theta_4)$ is a hyperspherical function on S_3.

3. Polyspherical to four-dimensional cylindrical coordinates on Fig.7(10) (see also Fig.7(10')) $[R \to \infty,\ J \sim kR,\ m_1 \sim k_1 R]$

$$\lim_{R\to\infty} \frac{1}{R} \Psi_{Jlm_1m_2}(\theta_1,\theta_2,\theta_3,\theta_4) = \sqrt{\frac{k}{\pi r}} e^{ik_1x_1} J_{l+1/2}(pr) Y_{lm_2}(\pi/2-\theta_3,\theta_4),$$

where $Y_{lm_2}(\pi/2-\theta_3,\theta_4)$ is a spherical function on S_2 and $k^2 = k_1^2 + p^2$.

4. Polyspherical to four-dimensional cylindrical coordinates on Fig.7(11) (see also Fig.7(11')) $[R \to \infty,\ J \sim kR,\ l \sim k_4 R]$

$$\lim_{R\to\infty} \frac{(-1)^{(J-l_1)/2}}{R} \Psi_{Jl_1l_2m}(\theta_1,\theta_2,\theta_3,\theta_4) = \sqrt{\frac{2pk}{\pi k_4 r}} J_{l_2+\frac{1}{2}}(pr) Y_{l_2m}(\theta_3,\theta_4) \left\{ \begin{array}{l} \cos(k_4x_4) \\ -i\sin(k_4x_4) \end{array} \right\},$$

where $Y_{l_2m}(\theta_3,\theta_4)$ is a spherical function on S_2 and $k^2 = k_4^2 + p^2$.

5. Polyspherical to bipolar coordinates on Fig.7(12) $[R \to \infty,\ J \sim kR,\ l \sim k_1 R]$

$$\lim_{R\to\infty} \frac{1}{R} \Psi_{Jlm_1m_2}(\theta_1,\theta_2,\theta_3,\theta_4) = \frac{\sqrt{2kk_1}}{2\pi} J_{m_1}(k_1r_1)\, J_{m_2}(k_2r_2) e^{im_1\theta_3 + im_2\theta_4}$$

where $k_1^2 + k_2^2 = k^2$.

6. Polyspherical to double cylindrical coordinates on Fig.7(13) (see also Fig.7(13')) $[R \to \infty,\ J \sim kR,\ l \sim k_1 R,\ m \sim k_2 R]$

$$\lim_{R\to\infty} \frac{(-1)^{(l-m_1)/2}}{\sqrt{R}} \Psi_{Jlm_1m_2}(\theta_1,\theta_2,\theta_3,\theta_4) = \sqrt{\frac{k\sqrt{k_1^2+k_2^2}}{\pi^3 k_2}} e^{ik_1x_1} \left\{ \begin{array}{l} \cos(k_2x_2) \\ -i\sin(k_2x_2) \end{array} \right\} J_{|m_2|}(k_3r) \frac{e^{im_2\theta_4}}{\sqrt{2\pi}}$$

where $k_1^2 + k_2^2 + k_3^2 = k^2$.

7. Polyspherical to double cylindrical coordinates on Fig.7(14) $[R \to \infty,\ J \sim kR,\ l_1 \sim k_3 R,\ l_2 \sim k_1 R]$

$$\lim_{R\to\infty} \frac{(-1)^{(J-l_2)/2}}{\sqrt{R}} \Psi_{Jl_1l_2m}(\theta_1,\theta_2,\theta_3,\theta_4) = \sqrt{\frac{2k_1k\sqrt{k_1^2+k_2^2}}{\pi^3 k_2 k_3}} J_{|m|}(k_1r) e^{im_2\theta_4} \left\{ \begin{array}{l} \cos k_3x_3 \cos k_4x_4 \\ -i\sin k_3x_3 \cos k_4x_4 \\ -i\cos k_3x_3 \sin k_4x_4 \\ -\sin k_3x_3 \sin k_4x_4 \end{array} \right\},$$

where $k_1^2 + k_2^2 + k_3^2 = k^2$.

8. Polyspherical to Cartesian coordinates on Fig.7(15) $[R \to \infty,\ J \sim kR,\ m \sim k_1 R,\ l_2 \sim k_2 R,\ l_1 \sim k_3 R]$

$$\lim_{R\to\infty} (-1)^{(J-m)/2} \Psi_{Jl_1l_2m}(\theta_1,\theta_2,\theta_3,\theta_4) = \sqrt{\frac{8k\sqrt{k_1^2+k_2^2}\sqrt{k_1^2+k_2^2+k_3^2}}{\pi^4 k_2 k_3 k_4}} e^{ik_1x_1} \times \left\{ \begin{array}{ll} \cos k_2x_2 \cos k_3x_3 \cos k_4x_4; & -i\sin k_2x_2 \cos k_3x_3 \cos k_4x_4; \\ -i\cos k_2x_2 \sin k_3x_3 \cos k_4x_4; & -\sin k_2x_2 \sin k_3x_3 \cos k_4x_4; \\ -i\cos k_2x_2 \cos k_3x_3 \sin k_4x_4; & -\sin k_2x_2 \cos k_3x_3 \sin k_4x_4; \\ -\cos k_2x_2 \sin k_3x_3 \sin k_4x_4; & -i\sin k_2x_2 \sin k_3x_3 \sin k_4x_4; \end{array} \right\},$$

where $k_1^2 + k_2^2 + k_3^2 + k_4^2 = k^2$.

As a final example let us consider the contraction $O(8) \to E(7)$ for the coordinate systems of Fig.3. The contraction of the $O(8)$ basis to the $E(7)$ one in this case is $[R \to \infty,\ l_1 \sim kR,\ l_2 \sim k_2 R,\ l_3 \sim k_1 R]$:

$$\lim_{R\to\infty} \frac{1}{R^2} \Psi_{l_1l_2l_3l_4l_5l_6l_7}(\theta_1,\theta_2,\theta_3,\theta_4,\theta_5,\theta_6,\theta_7) = \frac{\sqrt{k_2k_3}}{2\pi r_2} J_{|l_4|}(k_2r_1) J_{l_5+1}(k_3r_2) e^{ik_1x_1} e^{il_4\theta_4} Y_{l_5l_6l_7}(\theta_5,\theta_6,\theta_7).$$

7 Conclusion

In our previous paper [1] we studied contractions of all (i.e. both) coordinate systems on S_2 to all (four) coordinate systems on E_2. Here we have presented all possible contractions of subgroup type coordinate systems on S_n to subgroup type ones on E_n for n arbitrary. Moreover, we have developed a graphical formalism illustrating these contractions.

Contractions of ellipsoidal and **paraboloidal** coordinate systems will relate more "exotic" special functions amongst each other. For instance Lamé polynomials and their generalizations will go into Mathieu functions, parabolic cylinder functions, spheroidal functions etc. Work in this direction is in progress.

Fig.1. Subgroup type coordinates on S_n.

N	Subgroup chain	Subgroup diagram	Tree diagram
2	$O(2)$		
3.1	$O(3) \supset O(2)$		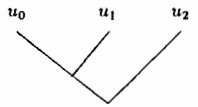
4.1	$O(4) \supset O(3) \supset O(2)$		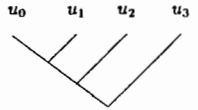
4.2	$O(4) \supset O(2) \otimes O(2)$	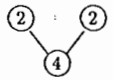	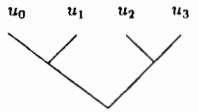
5.1	$O(5) \supset O(4) \supset O(3) \supset O(2)$		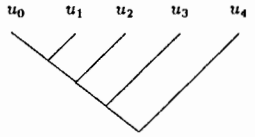
5.2	$O(5) \supset O(4) \supset O(2) \otimes O(2)$	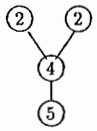	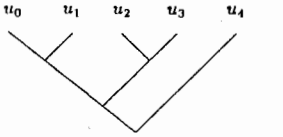
5.3	$O(5) \supset O(3) \otimes O(2) \supset O(2)$	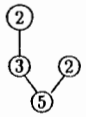	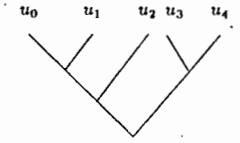

Fig.2. Equivalent tree diagrams corresponding to one subgroup diagram.

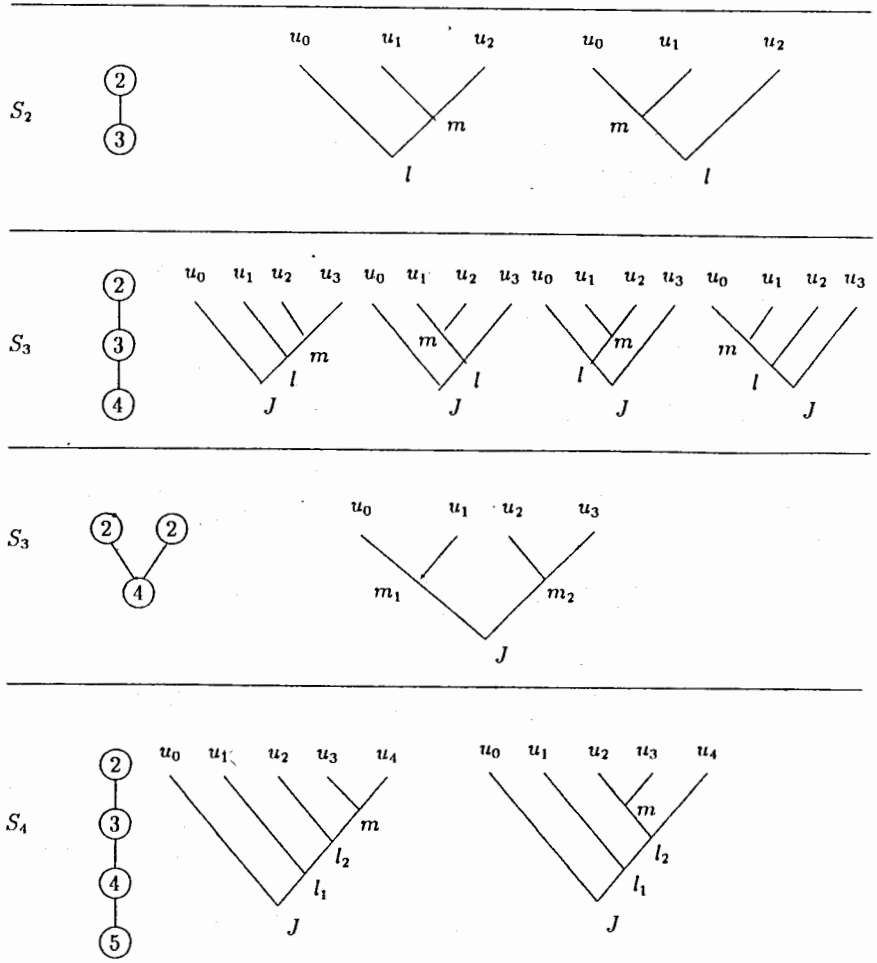

Fig.2. (continue)

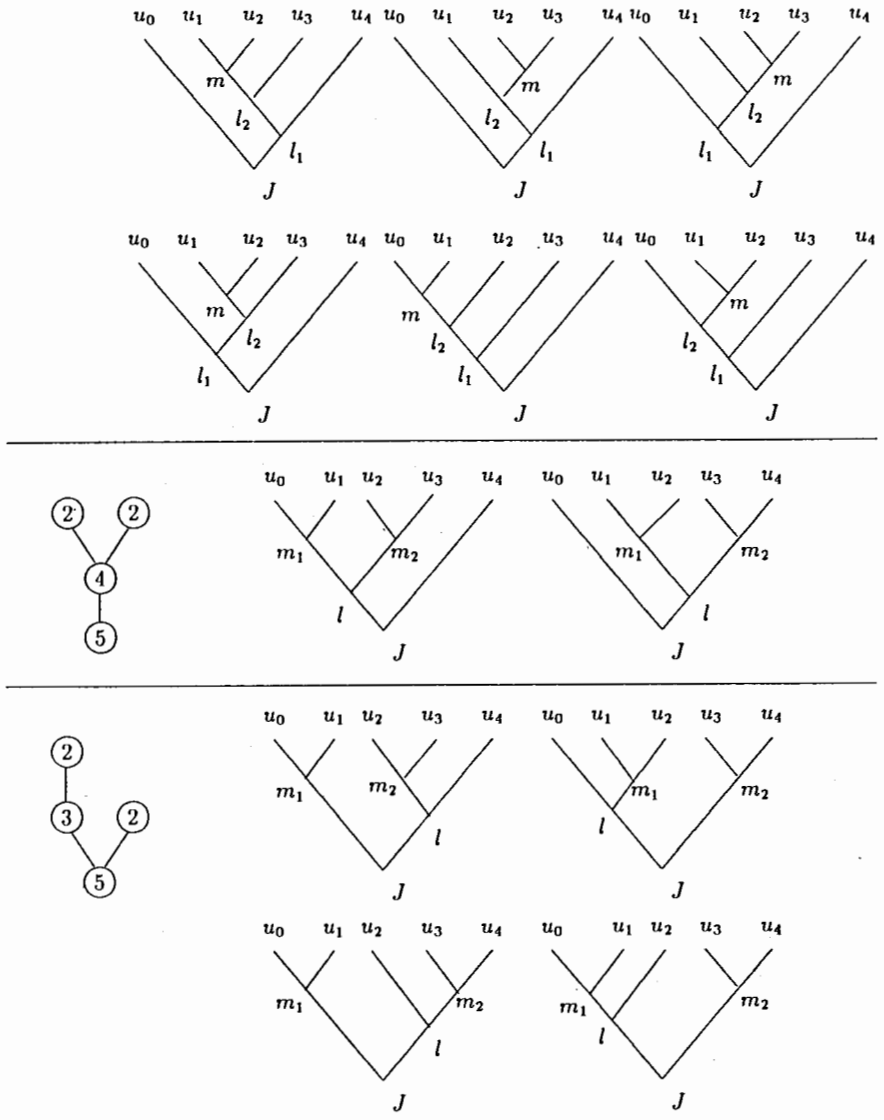

Fig.3. Example of an $O(8)$subgroup and S_7 tree diagram:

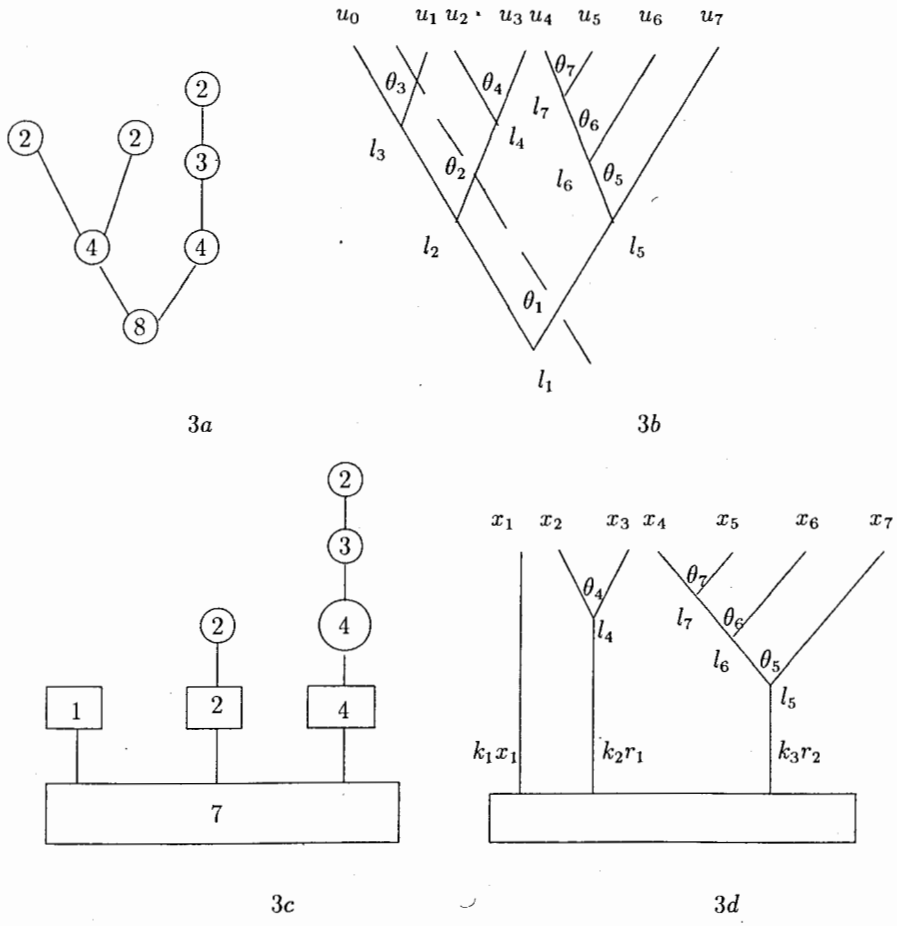

3a 3b

3c 3d

Fig.4 Elementary cells for S_n (diagrams $1a, \ldots, 1c$) and their contractions to E_n ones (diagrams $2a, \ldots, 2c$)

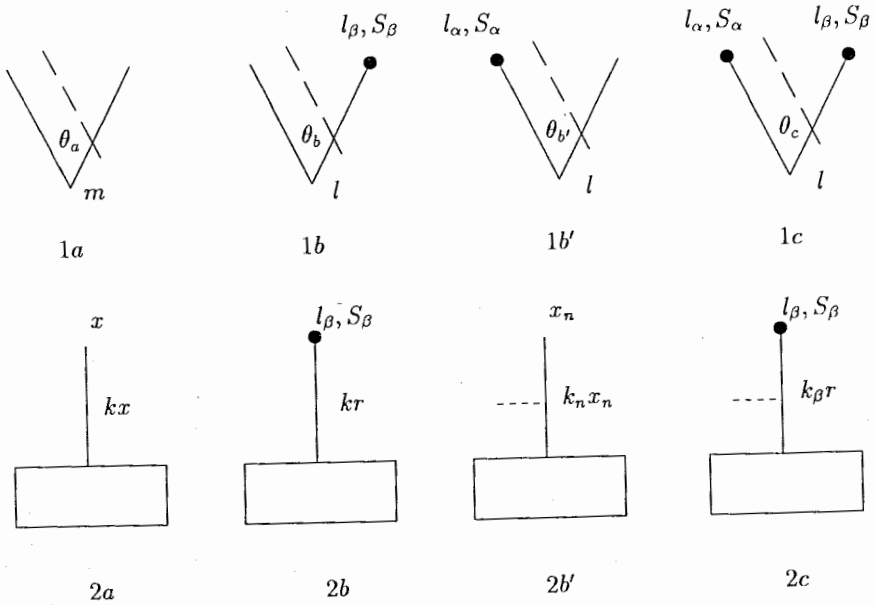

$1a$ $1b$ $1b'$ $1c$

$2a$ $2b$ $2b'$ $2c$

Fig.5. Subgroup chains for $E(n)$ and cluster diagrams on E_n.

Subgroup chain	Subgroup diagram	Cluster diagram
$E(1)$		
$E(2) \supset O(2)$		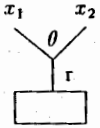
$E(2) \supset E(1) \otimes E(1)$	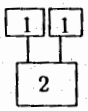	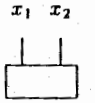
$E(3) \supset O(3) \supset O(2)$		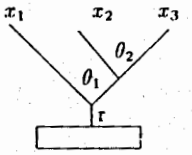
$E(3) \supset E(2) \otimes E(1) \supset O(2)$	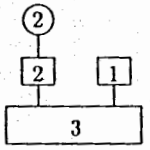	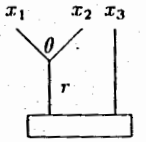
$E(3) \supset E(2) \otimes E(1) \supset E(1) \otimes E(1)$	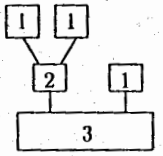	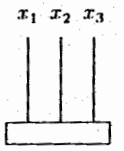
$E(4) \supset O(4) \supset O(3) \supset O(2)$	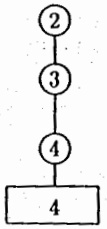	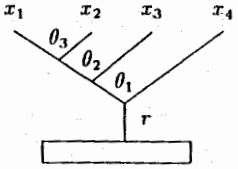

Fig.5. (continue)

$E(4) \supset O(4) \supset O(2) \otimes O(2)$

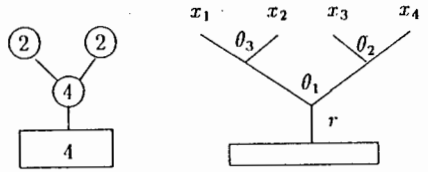

$E(4) \supset E(3) \otimes E(1) \supset O(3) \supset O(2)$

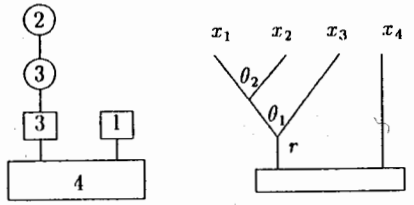

$E(4) \supset E(2) \otimes E(2) \supset O(2) \otimes O(2)$

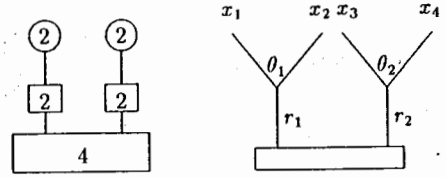

$E(4) \supset E(3) \otimes E(1) \supset E(2) \otimes E(1) \supset O(2)$

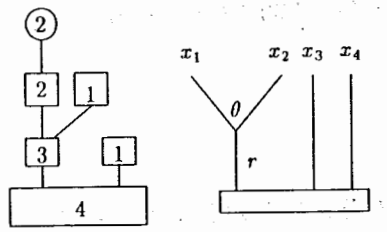

$E(4) \supset E(2) \otimes E(2) \supset O(2) \otimes E(1) \otimes E(1)$

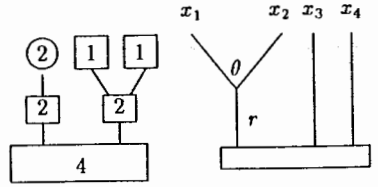

Fig.5. (continue)

$E(4) \supset E(3) \otimes E(1) \supset$

$E(2) \otimes E(1) \supset E(1) \otimes E(1)$

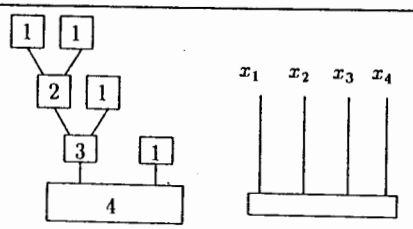

$E(4) \supset E(2) \otimes E(2) \supset$

$E(1) \otimes E(1) \otimes E(1) \otimes E(1)$

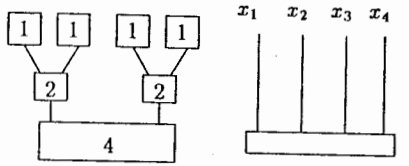

Fig.6. Contractions of tree diagrams into cluster ones for S_n.

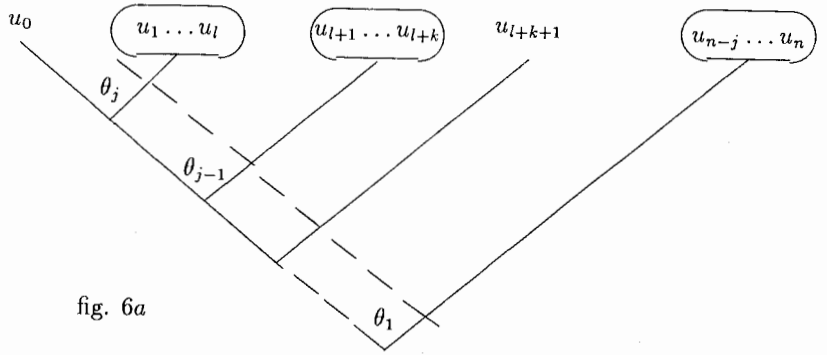

fig. 6*a*

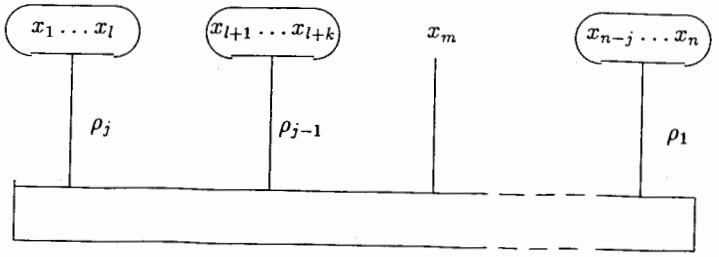

fig. 6*b*

Fig.7. Contractions of tree diagrams into cluster for $1 \leq n \leq 4$.

N	Cut tree diagram	Cluster diagram	Contraction of coordinates
1			Polar to Cartesian
2	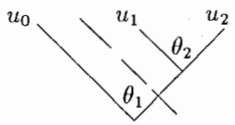	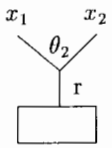	Spherical to Spherical
3	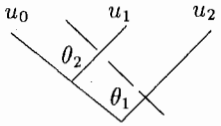	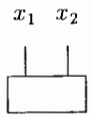	Spherical to Cartesian
4	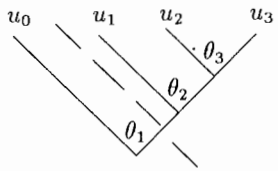	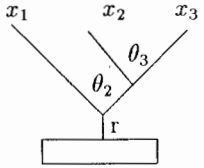	Spherical to Spherical
4′	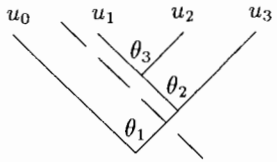	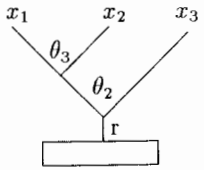	Spherical to Spherical
5	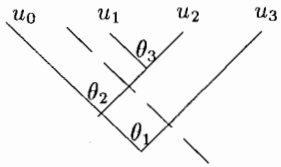	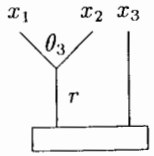	Spherical to Cylindrical

Fig.7. (continue)

6	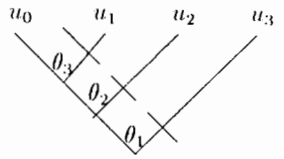	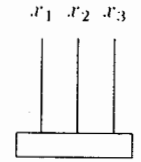 Spherical to Cartesian
7	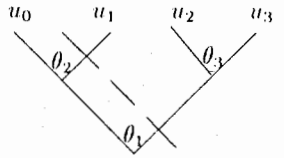	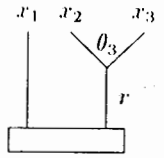 Cylindrical to Cylindrical
8	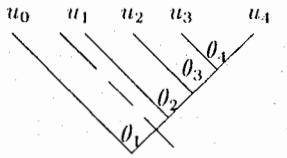	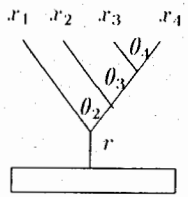
8′	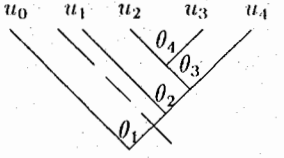	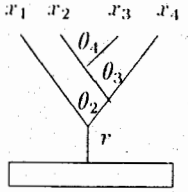
8″	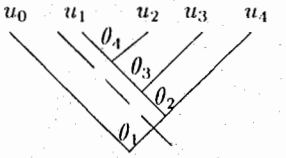	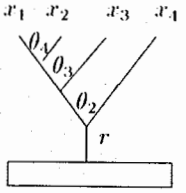
8‴	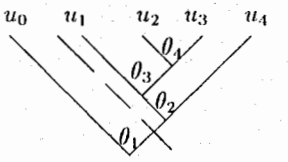	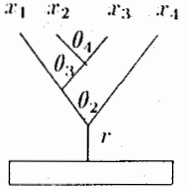

Fig.7. (continue)

9

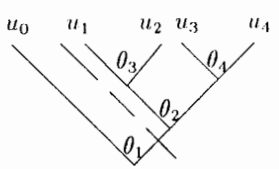

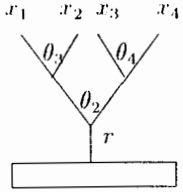

10

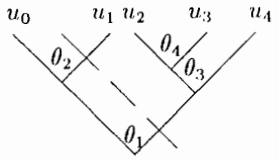

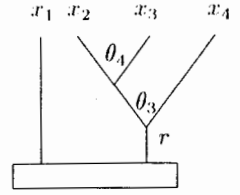

10′

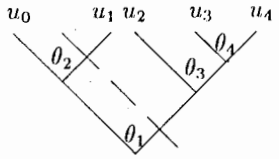

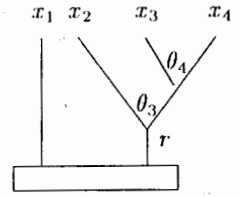

11

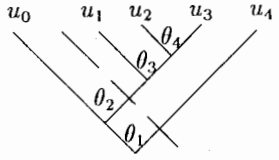

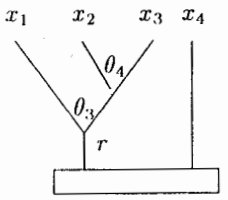

11′

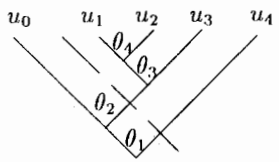

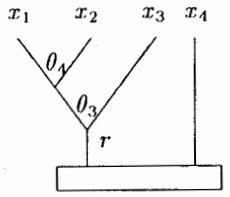

Fig.7. (continue)

12

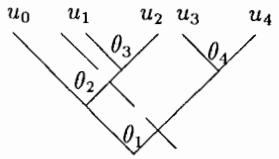

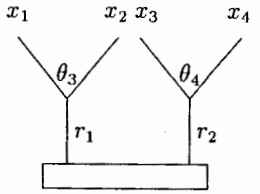

13

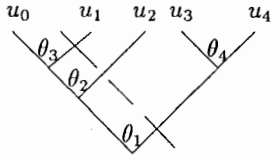

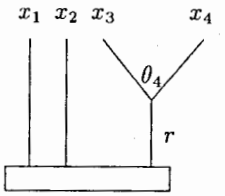

13′

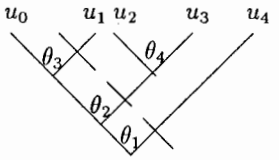

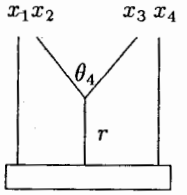

14

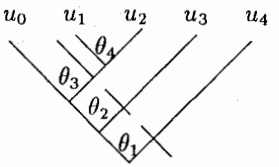

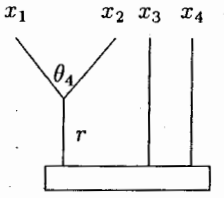

15

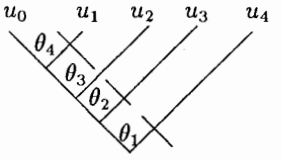

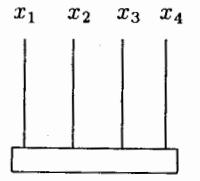

Acknowledgements

We thank Professors E. G. Kalnins, W. Miller Jr., and V. M. Ter-Antonyan for their interest and helpful discussions. We tank also Ye. M. Hakobyan for her help in the preparation of the diagrams. Two of the authors (G. P. and P. W.) thank each others institutions for hospitality during mutual visits that made the research leading to the present article possible.

The research of P. W. was partially supported by research grants from NSERC of Canada and FCAR du Québec.

References

[1] A. A. Izmest'ev, G. S. Pogosyan, A. N. Sissakian and P. Winternitz, *Contractions of Lie algebras and separation of variables*, J. Phys. **A29**, 5940–5962, (1996).

[2] A.A.Izmest'ev, G. S. Pogosyan, A. N. Sissakian and P. Winternitz, *Contractions of Lie algebras and separation of variables. Two-dimensional hyperboloid*, Inter. J. Mod. Phys. **A12**, 53–61, (1997).

[3] P. Winternitz and I. Fris, *Invariant expansions of relativistic amplitudes and subgroups of the proper Lorentz group*, Sov. J. Nucl. Phys. **1**, 636–643, (1965) [Yad. Fiz., **1**, 889–901, (1965)].

[4] P. Winternitz, I. Lukac, and Ya. A. Smorodinskii, *Quantum numbers in the little groups of the Poincaré group*, Sov. J. Nucl. Phys. **7**, 139-145, (1968) [Yad. Fiz., **7**, 192–201, (1968)].

[5] J. Patera and P. Winternitz, *A new basis for representations of the rotation group. Lamé and Heun polynomials*, J. Math. Phys. **14**, 1130–1139, (1973).

[6] W. Miller, Jr., J. Patera, and P. Winternitz, *Subgroups of Lie groups and separation of variables*, J. Math. Phys. **22**, 251–260, (1991).

[7] W. Miller, Jr., *Symmetry and Separation of Variables* (Addison-Wesley, Reading, MA, 1997).

[8] E. G. Kalnins, *Separation of Variables for Riemannian spaces of constant curvature* (Longman, Burnt Mill, 1986).

[9] N. Ya. Vilenkin, ıPolyspherical and orispherical functions, Mat. Sbornik, 68 (110), 432–443, (1965).

[10] N. Ya. Vilenkin, *Special Functions and the Theory of Group Representations* (Am. Math. Soc., Providence, RI 1968)

[11] N. Ya. Vilenkin, G. I. Kuznetsov and Ya. A.Smorodinskii, *Eigenfunctions of the Laplace operator realizing representations of the groups $U(2)$, $SU(2)$, $SO(3)$, $U(3)$ and $SU(3)$ and the symbolic method*, Sov. J. Nucl. Phys. **2**, 645–655, (1965) [Yad. Fiz., **2**, 906–917, (1965)].

[12] M. S. Kildyushov, *Hyperspherical functions of the "tree" type in the n-particle problem*, Sov. J. Nucl. Phys. **15**, 113–123, (1972) [Yad. Fiz. **15**, 197–208 (1972)].

[13] G. I. Kuznetsov, S. S. Moskalyuk, Yu. F. Smirnov and V. P. Shelest, *A Graphical theory of representations of orthogonal and unitary groups and its physical applications*, (Kiev, Naukova Dumka, 1992) (in Russian).

[14] E. Inönü and E. P. Wigner, *On the contraction of groups and their representations*, Proc. Nat. Acad. Sci. (US) **39**, 510–524, (1953).

[15] E. J. Saletan, *Contraction of Lie groups*, J. Math. Phys. **2**, 1–21, (1961).

[16] R. Gilmore, *Lie Groups, Lie Algebras and Some of their Applications* (Wiley, New York, 1974).

[17] R. V. Moody and J. Patera, *Discrete and continuous graded contractions of representations of Lie algebras*, J. Phys. **A24**, 2227 2258, (1991).

[18] X. Leng and J. Patera, *Graded contractions of representations of $sl(n,C)$ with respect to the maximal parabolic subalgebras*, J. Phys. **A27**, 1233-1250, (1987).

[19] M. Couture, J. Patera, R. T. Sharp, and P. Winternitz, *Graded contractions of $sl(3,C)$* J. Math. Phys. **32**, 2310–2318, (1991).

[20] M. Ait Abdelmalek, X. Leng, J. Patera and P. Winternitz, *Grading refinements in the contractions of Lie algebras and their invariants*, J. Phys. **A29**, 7519 7543, (1996).

[21] P. Winternitz, *Successive refinements of gradings and graded contractions of $sl(3,C)$*, Intern. J. Mod. Phys. **A12**, 109 115, (1997).

[22] J. Patera, G. Pogosyan, and P. Winternitz, *Graded contractions of the Lie algebra $e(2,1)$*, CRM-2484, (1997).

[23] E. Weimar-Woods, *Contractions of Lie algebras: generalized Inönü-Wigner contractions versus graded contractions*, J. Math. Phys. **36**, 4519 4548, (1995).

[24] L. P. Eisenhart, *Separable systems of Stäckel*, Ann.Math. **35**, 284-305, (1934).

[25] D. A. Suprunenko and R. I. Tyshkevich, *Commutative matrices*, (Academic, New-York, 1968).

[26] J. Patera, P. Winternitz and H. Zassenhaus, *Maximal Abelian subalgebras of real and complex symplectic Lie algebras*, J.Math.Phys. **24**, 1973–1985, (1983).

[27] M. A. del Olmo, M. A. Rodriguez, P. Winternitz, and H. Zassenhaus, *Maximal Abelian subalgebras of pseudounitary Lie algebras*, Lin. Alg. Appl. **135**, 79–151, (1990).

[28] V. Hussin, P. Winternitz, and H. Zassenhaus. *Maximal Abelian subalgebras of complex orthogonal Lie algebras*, Lin. Alg. Appl. **141**, 183-220, (1990).

[29] V. Hussin, P. Winternitz, and H. Zassenhaus, *Maximal Abelian subalgebras of pseudoorthogonal Lie algebras*, Lin. Alg. Appl. **173**, 125–163, (1992).

[30] E. G. Kalnins, and P. Winternitz, *Maximal Abelian subalgebras of complex Euclidean Lie algebras*, Canad. J. Phys. **72**, 389–404, (1994).

[31] Z. Thomova and P. Winternitz, *Maximal Abelian subgroups of the isometry and conformal groups of Euclidean and Minkowski spaces*, J.Phys **A31**, 1831–1859, (1998).

[32] M. N. Olevskii, *Orthogonal systems in spaces of constant curvature in which the equation* $\Delta_2 u + \lambda u = 0$ *allows a complete separation of variables*, Math. Sbornik, **27** (69), 379–426, (1950) (in Russian).

[33] E. Kalnins, W. Miller, Jr., and P. Winternitz, *The group* $O(4)$*, separation of variables and the hydrogen atom*, SIAM J. Appl. Math. **30**, 630–664, (1976).

[34] V. A. Knyr, P. P. Pepiraite, and Yu. F. Smirnov, *Canonical transformations, "trees" and momenta divisible by* 1/4, Sov. J. Nucl. Phys. **22**, 554, (1975) [Yad. Fiz. **22**, 1063 (1975)].

[35] S. K. Suslov, *The T-coefficients of the "tree" method as orthogonal polynomials of discrete variable*, Sov. J. Nucl. Phys. **38**, 829–833, (1983) [Yad. Fiz. **38**, 1367–1375 (1983)].

[36] G. I. Kuznetsov and Ya. A. Smorodinskii, *Hyperspherical Trees and 3nj-coefficients*, Pis'ma v JETF **22**(7), 378–380 (1975) (in Russian).

[37] W. N. Bailey, *Generalized hypergeometric series*, (Cambridge Tracts, No 32, Cambridge 1935).

[38] G. Bateman, A. Erdélyi, *Higher Transcendental Functions*, (McGraw-Hill Inc, New York, 1953).

[39] D. A. Varshalovich, A. N. Moskalev and V. K. Khersonskii, *Quantum Theory of Angular Momentum*, (Nauka, Leningrad, 1975).

Received by Publishing Department
on March 18, 1998.